OPEN JOURNAL SYSTEMS
ISSN:2237-2202

Available on line at Directory of Open Access Journals
Journal of Hyperspectral Remote Sensing v.12, n.6 (2022) 379-390

www.periodicos.ufpe.br/revistas/jhrs

Journal of Hyperspectral Remote Sensing
www.ufpe.br/jhrs

Quantitative differences in detection of fire pixels using Aqua/MODIS and NPP-Suomi/VIIRS satellites

***Benjamin Leonardo Alves White**

*Instituto Federal Baiano, Campus Xique-Xique, Rodovia BA 052, Km 468, Xique-Xique, Bahia, Brasil
E-mail: benjamin.white@ifbaiano.edu.br
Orcid: https://orcid.org/0000-0001-8491-1853

Received 7 November 2022; accepted 13 December 2022

Abstract
Since 2002, the AQUA (MODIS) satellite has been used as a "reference" by the Brazilian National Institute of Space Research to analyze spatial and temporal trends over fire pixel detection in all South America. Since this satellite will stop providing data in the near future, in order to continue the trend analyzes it will be necessary an integration and adjustment between AQUA fire pixels data with the data from the next reference satellite: the Suomi NPP (VIIRS). Therefore, this study has as objective to analyze the differences in fire pixels detection from AQUA and S-NPP satellites at country, state and municipal level. During the 10 years period assessed, the S-NPP detected, on average, 5.13 times more fire pixels than the AQUA on the South America continent. Venezuela was the country with the highest S-NPP/AQUA ratio (6.81) and Chile the lowest (3.87). When analyzing the fire pixels only in the Brazilian states, Acre presented the lowest S-NPP/AQUA ratio (3,72), while in Sergipe the highest (10,07). In the Pará's municipalities, the lowest S-NPP/AQUA ratio was in Quatipuru (2.84), while the highest in Ananindeua (11.25). Despite the differences in the ratio, the number of fire pixels detected by the AQUA and S-NPP presented, almost in all cases, a significant correlation. Only the smallest municipalities in Pará had no significant correlation, probably due to low data and/or detection location errors. The changes in the S-NPP/AQUA ratio occurred probably due to factors such as sampling characteristics (pixel enlargement away from nadir), geographic area analyzed, timing of satellite overpasses, predominant type of vegetation, and others. Therefore, there isn't one unique formula to adjust AQUA data to S-NPP, variations will persist at different locations.
Keywords: wildland fire; remote sensing; fire prevention.

Statements and declarations

This study was developed without any financial interest.

Conflict of interest

There is no conflict of interest.

Diferenças quantitativas na detecção de pixels de fogo usando os satélites Aqua/MODIS e NPP-Suomi/VIIRS

RESUMO

Desde 2002, o satélite AQUA (MODIS) tem sido usado como “referência” pelo Instituto Nacional de Pesquisas Espaciais do Brasil para analisar tendências espaciais e temporais na detecção de pixels de fogo em toda a América do Sul. Uma vez que este satélite deixará de fornecer dados em um futuro próximo, para continuar as análises de tendências, será necessária uma integração e ajuste entre os dados de pixels de fogo AQUA com os dados do próximo satélite de referência: o Suomi NPP (VIIRS). Portanto, este estudo tem como objetivo analisar as diferenças na detecção de pixels de incêndio dos satélites AQUA e S-NPP em nível nacional, estadual e municipal. Durante o período de 10 anos avaliado, o S-NPP detectou, em média, 5,13 vezes mais pixels de incêndio do que o AQUA no continente sul-americano. A Venezuela foi o país com a maior relação S-NPP/AQUA (6,81) e o Chile a menor (3,87). Ao analisar os pixels de fogo apenas nos estados brasileiros, o Acre apresentou a menor relação S-NPP/AQUA (3,72), enquanto em Sergipe a maior (10,07). Nos municípios paraenses, a menor relação S-NPP/AQUA foi em Quatipuru (2,84), enquanto a maior em Ananindeua (11,25). Apesar das diferenças na proporção, o número de pixels de incêndio detectados pelo AQUA e S-NPP apresentou, quase em todos os casos, uma correlação significativa. Apenas os menores municípios do Pará não tiveram correlação significativa, provavelmente devido a poucos dados e/ou erros de localização de detecção. As mudanças na relação S-NPP/AQUA ocorreram provavelmente devido a fatores como características da amostragem (alargamento dos pixels a partir do nadir), área geográfica analisada, tempo de passagem dos satélites, tipo de vegetação predominante, entre outros. Portanto, não há uma fórmula única para ajustar os dados AQUA para S-NPP, as variações persistirão em diferentes locais.

Palavras-chave: incêndio florestal; sensoriamento remoto; Prevenção de incêndio.

1.Introduction

Technological advances have enabled the use of satellite remote sensing to detect and locate fires in real time since 1980s (Caula et al., 2015; Wang et al., 2012). Until a few years ago, the satellites equipped with Advanced Very High-Resolution Radiometer (AVHRR) and Moderate Resolution Imaging Spectroradiometer (MODIS) sensors were the most effective for this purpose (White 2020). Two new satellites launched in the 2010s, the Suomi National Polar-orbiting Partnership (S-NPP) and the National Oceanic and Atmospheric Administration (NOAA-20) equipped with the Visible Infrared Imaging Radiometer Suite (VIIRS) sensor, are currently the most efficient due to their greater resolution capacity (INPE, 2022; White, 2020). Nevertheless, data from older satellites still in operation, continue to be used to analyze longer term variations in fire occurrence (White 2020; INPE 2022).

Satellite fire detection is performed using algorithms that measures the emission of mid-infrared radiation from fires (GIGLIO et al. 2006). Initially, obvious non-fire pixels are excluded. For those remain potential fire pixels, the neighboring pixels are used to estimate the radiometric signal of the potential fire pixel in the absence of fire. Then, a series of contextual threshold tests are used to perform a relative fire detection where characteristic signature of an active fire in which both 4 µm brightness temperature and the 4 and 11 µm brightness temperature difference depart substantially from that of the non-fire background (Giglio et al., 2018). Additional specialized tests are used to eliminate false detections caused by sun glint, desert boundaries, errors in the water mask, and small forest clearings. Pixels that are not rejected in the course of applying these tests are assigned as active fire pixels (Giglio et al., 2018).

Since 1998, the Brazilian National Institute for Space Research (INPE), started to receive data from satellites capable of detecting active fire pixels to monitor wildland fire occurrence in Brazil and all South America. Although receiving data from several satellites, the INPE used, from June 1, 1998 to July 3, 2002, the satellite NOAA-12 (AVHRR sensor, afternoon passage), and from then on, the AQUA (MODIS sensor, afternoon passage), as “reference” satellites. By using the same detection method and generating images at similar times over the years, the data from the reference satellites allow analyzing the spatial and temporal trends of the fire pixels, thus enabling trend analyzes for the same periods in regions of interest (White, 2018; INPE, 2022). Such data from the reference satellites, mostly from the AQUA, have already been used by several researchers to describe the spatiotemporal variation of wildland fire occurrence at global level (eg. Csiszar et al., 2005; Giglio et al., 2006), at continental level (eg. Csiszar et al., 2006; White, 2019), at country level (eg. Matin et al., 2017; Hawbaker, 2008; Xia et al., 2013); at state level (eg. Badarinath et al., 2011; White and White, 2016; White, 2018; White, 2020), and at municipal level (eg. White and White, 2016; White, 2018; White, 2020). These studies are essential for the efficient development of specific strategies and public policy focused on fire fighting and prevention.

The both satellites equipped with MODIS sensor (AQUA and TERRA) have far exceeded their expected lifespan, and will stop working in the near future. So, it will be necessary an integration and adjustment between MODIS data with the data from the next reference satellite, that, according to INPE (2022), will be the S-NPP (VIIRS sensor, afternoon passage). Since AQUA and S-NPP have similar overpass times and both observe the earth two times during the day (morning and afternoon), sampling of the diurnal fire cycle is similar (INPE, 2022).

Initially, the S-NPP active fire detection products was based only on the 750 m (M-bands) nominal resolution, which was evolved from the baseline algorithm implementation designed to provide continuity to the 1-km MODIS active fire data record. During the early post-launch period, the satellite 375 m (I-bands) channels, where repurposed for fire detection, since none of these channels were originally designed for this function (Schroeder and Giglio, 2017). To process the images generated with this new resolution, a new algorithm (VNP14IMG) was developed. This algorithm is based on a similar evolving MODIS baseline product, thus ensuring the ability to support data continuity between the products derived from the MODIS and VIIRS missions (NASA, 2022).

The algorithm currently used by the INPE and by the National Aeronautics and Space Administration (NASA) to detect active fire pixels in MODIS images is the MOD14/MYD14 Fire and Thermal Anomalies algorithm. The last updated MODIS fire pixels data come from the Collection 6.1 version, that consist in a reprocessing of the entire MODIS data archive from the previous version (Collection 5) (NASA, 2022). Such update is periodically performed to incorporate better calibration, algorithm refinements, and improved upstream data into all MODIS products. Later collections supersede all earlier collections (Giglio et al., 2018).

Despite the similarities between MODIS and VIIRS fire products, compared to the 1-km MODIS bands for fire detection, the VIIRS higher spatial resolution (375 m) enables the detection of smaller and cooler fires, as well as improved mapping of large fire perimeters (Csiszar et al., 2014; Li et al., 2018; Schroeder and Giglio, 2017). VIIRS also applies onboard aggregation processing to compensate for pixel footprint enlargement with distance from nadir, which strongly affects its fire detection data (Cao et al., 2013; Schroeder et al., 2014).

To continue the analyzes of wildland fire occurrence trends over Brazil and all South America, it is essential to understand the similarities and discrepancies between the data collect ed from both satellites (AQUA and S-NPP) during their overlap period, in order to properly built an adjustment model. Until now, there are only a few studies comparing data from those satellites and none of them concern fire pixels in Brazil or South America. Therefore, this study’s objective is to compare, analyze and discuss the differences in the number of fire pixels detected from the AQUA 1-km MODIS and S-NPP VIIRS 375 m sensors from January 1, 2012 to December 31, 2021, totaling 10 years of data.

2.Methods

Data of fire pixels detected from 2012 to 2021 was obtained at the INPE Satellite Monitoring Burning Program website using AQUA satellite (afternoon passage), and the S-NPP satellite (afternoon passage). The AQUA data is based on NASA MODIS Collection 6 fire product, and the S-NPP based on NASA VIIRS I Band 375 m Active Fire Product NRT (VNP14IMGTDL_NRT).

The comparison was done at country level (in all South America countries), at state level (in all Brazilian states) and at municipal level (in all municipalities of the Pará state). Brazil and the state of Pará were chosen because they are the country and state, respectively, that have the highest annual averages of fire pixels detected since satellite monitoring began in South America (INPE, 2022).

All data collect were first grouped according to the year and the site where the fire pixels were detected, then had their mean and standard deviation values determined. The total number of fire pixels detected by the S-NPP was divided by the AQUA, for each location assessed, in order to determine the S-NPP/AQUA ratio. The Pearson correlation coefficient (r) was used to assess the yearly correlation between both satellite data. Adjustment models from S-NPP data to AQUA data, or vice-versa, were built using linear regression and had their coefficient of determination (r^2) calculated.

3.Results

During the 10 years evaluated, 17,037,769 fire pixels were detected by the S-NPP in South America, while the AQUA detected 3,324,070 at the same location. Of these values, 9,502,181 and 1,867,154 fire pixels where detected in Brazil by the S-NPP and AQUA, respectively. In the state of Pará, the S-NPP detected 1,531,636 and the AQUA 333,175 (Table 1).

Table 1 – Number of fire pixels detected in South America, Brazil and Pará by the AQUA and S-NPP satellites between 2012-2021.

	S-NPP	**AQUA**	**S-NPP/AQUA ratio**
Fire pixel detected in South America 2012-2021	17,037,769	3,324,070	5.13
Fire pixel detected in Brazil 2012-2021	9,502,181	1,867,154	5.09
Fire pixel detected in Pará 2012-2021	1,531,636	333,175	4.60

Analyzing the South America countries individually, it was noticed that Venezuela had the highest S-NPP/AQUA ratio and Chile the lowest. All countries presented a significant correlation between the number of fire pixels detected yearly by the S-NPP and the AQUA ($p<0.01$). The one with the lowest correlation coefficient was Peru, but still highly significant ($r = 0.926$; $p < 0.01$) (Tabel 2).

Table 2 – List of South America countries arranged in descending order of significance according the Pearson correlation coefficient between the yearly number of fire pixels detected by the AQUA and S-NPP satellites. Also, are presented the S-NPP/AQUA ratio, the adjusted linear regression equations for each country and their respective coefficient of determination. The highest and lowest S-NPP/AQUA ratio are highlighted in bold.

South America country	**S-NPP/AQUA ratio**	**Pearson correlation (r)**	**Linear regression equation**	**Coefficient of determination (r^2)**
Argentina	4,31	0.994	S-NPP = -14227,56 + 4,72*AQUA	0.989
Brazil	5,09	0.994	S-NPP = -41923,86 + 5,31*AQUA	0.988
Bolivia	5,02	0.991	S-NPP = -10727,49 + 5,40*AQUA	0.981
Venezuela	**6,81**	0.990	S-NPP = -12951,54 + 7,38*AQUA	0.980
Paraguay	4,61	0.987	S-NPP = -1739,94 + 4,69*AQUA	0.975
Uruguay	4,21	0.976	S-NPP = 593,95 + 3,32*AQUA	0.952
Chile	**3,87**	0.975	S-NPP = -2337,5 + 4,47*AQUA	0.951
Guyana	6,68	0.974	S-NPP = 1103,33 + 5,75*AQUA	0.948
Colombia	5,68	0.966	S-NPP = -7998,42 + 6,16*AQUA	0.933
Suriname	5,23	0.955	S-NPP = -95,01 + 5,44*AQUA	0.912
French Guiana	4,92	0.950	S-NPP = 71,76 + 4,21*AQUA	0.901
Ecuador	6,58	0.946	S-NPP = 2679,09 + 5,33*AQUA	0.896
Peru	5,38	0.926	S-NPP = 14445,53 + 4,20*AQUA	0.857

When analyzing the fire pixels in Brazilian states, Acre presented the lowest S-NPP/AQUA ratio (3,72), while in Sergipe was recorded the highest value (10,07). The mean S-NPP/AQUA ratio was 5.09, very close to the South America ratio (5.13). All states presented a significant correlation between the number of fire pixels detected yearly by the S-NPP and the

AQUA ($p<0.01$). The one with the lowest correlation coefficient was Paraná, but still highly significant ($r = 0.953$; $p < 0.01$) (Table 3).

Table 3 - List of Brazilian states arranged in descending order of significance according the Pearson correlation coefficient between the yearly number of fire pixels detected by the AQUA and S-NPP satellites. Also, are presented S-NPP/AQUA ratio, the adjustment linear regression equations for each state and their respective coefficient of determination. The highest and lowest S-NPP/AQUA ratio are highlighted in bold.

Brazilian States	S-NPP/AQUA ratio	Pearson correlation (r)	Linear regression equation	Coefficient of determination (r^2)
Mato Grosso	4.81	0.998	S-NPP = -13749.53 + 5.30*AQUA	0.997
Bahia	5.82	0.998	S-NPP = 4382.05 + 5.36*AQUA	0.996
Mato Grosso do Sul	5.21	0.997	S-NPP = -954.25 + 5.36*AQUA	0.995
Tocantins	6.20	0.996	S-NPP = -6840.87 + 6.71*AQUA	0.992
Piauí	6.31	0.995	S-NPP = 3403.72 + 5.97*AQUA	0.991
Amapá	4.89	0.994	S-NPP = 463.58 + 4.62*AQUA	0.988
Acre	**3.72**	0.993	S-NPP = 878.93 + 3.59* AQUA	0.986
Rio Grande do Sul	4.99	0.990	S-NPP = 2508.91 + 3.94*AQUA	0.981
Roraima	6.29	0.990	S-NPP = 1404.52 + 5.68*AQUA	0.979
Distrito Federal	5.05	0.988	S-NPP = 107.35 + 4.49*AQUA	0.976
Espírito Santo	5.55	0.988	S-NPP = 288.13 + 4.90*AQUA	0.976
Alagoas	8.40	0.987	S-NPP = 540.75 + 6.22*AQUA	0.975
Paraíba	7.54	0.985	S-NPP = 967 + 6.08*AQUA	0.971
Minas Gerais	5.00	0.984	S-NPP = 4118.74 + 4.52*AQUA	0.968
Pará	4.60	0.984	S-NPP = -11441.95 + 4.94*AQUA	0.968
São Paulo	4.26	0.983	S-NPP = 1049.08 + 3.97*AQUA	0.967
Ceará	5.21	0.982	S-NPP = 3371.20 + 4.27*AQUA	0.965
Sergipe	**10.07**	0.980	S-NPP = 324.11 + 7.75*AQUA	0.960
Amazonas	4.16	0.979	S-NPP = -3500.86 + 4.46*AQUA	0.960
Maranhão	5.52	0.978	S-NPP = -7961.44 + 5.89 *AQUA	0.956
Rondônia	4.40	0.977	S-NPP = -634.54 + 4.46*AQUA	0.954
Rio de Janeiro	5.40	0.976	S-NPP = 440.298 + 4.73*AQUA	0.952
Goiás	5.95	0.968	S-NPP = -1008.14 + 6.13*AQUA	0.938
Pernambuco	7.92	0.964	S-NPP = 1851.75 + 5.77*AQUA	0.930
Santa Catarina	4.39	0.961	S-NPP = 1953.88 + 3.31*AQUA	0.923
Rio Grande do Norte	6.86	0.956	S-NPP = 515.83 + 5.72*AQUA	0.917
Paraná	4.16	0.953	S-NPP = 2617.56 + 3. 3*AQUA	0.909

In Pará municipalities, the lowest S-NPP/AQUA ratio was detected in Quatipuru (2.84), while the highest in Ananindeua (11.25). The mean S-NPP/AQUA ratio was 4.6, lower than the mean ratio for Brazil and South America.

Of the 144 Pará's municipalities, 122 presented significative Pearson correlation between AQUA and NPP yearly data at $p<0.01$. Another 8 municipalities presented significative correlation at $p<0.05$, while 14 presented no significative correlation ($p>0.05$) (Table 4).

Table 4 - List of Pará municipalities arranged in descending order of significance according Pearson correlation coefficient between the yearly number of fire pixels detected by the AQUA and S-NPP satellites. Also, are presented S-NPP/AQUA ratio, the adjustment linear regression equations for each municipality and their respective coefficient of determination. The highest and lowest S-NPP/AQUA ratio are highlighted in bold.

Pará municipality	S-NPP/AQUA ratio	Pearson correlation (r)	Linear regression equation	Regression coefficient (r^2)

São Félix do Xingu	4.99	0,997	S-NPP = -257,68 + 5,07*AQUA	0.994
Altamira	4.83	0,995	S-NPP = -1256,08 + 5,26*AQUA	0.990
Santa Maria das Barreiras	5.72	0,995	S-NPP = -421,38 + 6,39*AQUA	0.989
Conceição do Araguaia	5.47	0,993	S-NPP = -258,46 + 6,24*AQUA	0.987
Cumaru do Norte	5.84	0,993	S-NPP = -610,55 + 6,89*AQUA	0.986
Itaituba	4.03	0,989	S-NPP = -309,86 + 4,28*AQUA	0.977
Canaã dos Carajás	5.65	0,987	S-NPP = 19,36 + 5,42*AQUA	0.973
Novo Progresso	4.59	0,987	S-NPP = -525,57 + 4,9*AQUA	0.973
Abaetetuba	4.01	0,981	S-NPP = 144,67 + 2,82*AQUA	0.963
Santana do Araguaia	5.46	0,980	S-NPP = -346,41 + 6,16*AQUA	0.960
Eldorado do Carajás	5.04	0,977	S-NPP = 78,17 + 4,31*AQUA	0.954
Chaves	5.25	0,976	S-NPP = 134,56 + 4,45*AQUA	0.953
Jacareacanga	4.07	0,975	S-NPP = -151,62 + 4,32*AQUA	0.950
Trairão	3.9	0,974	S-NPP = -273,13 + 4,42*AQUA	0.948
Redenção	5.2	0,973	S-NPP = 63,70 + 4,61*AQUA	0.947
São João do Araguaia	5.51	0,973	S-NPP = 22,19 + 5,08*AQUA	0.947
Xinguara	5.17	0,971	S-NPP = -32,54 + 5,69*AQUA	0.943
Almeirim	4.39	0,970	S-NPP = -93,74 + 4,69*AQUA	0.941
Curionópolis	5.78	0,970	S-NPP = 29,73 + 5,26*AQUA	0.940
Marabá	5.06	0,969	S-NPP = 306,79 + 4,45*AQUA	0.938
Anajás	5.51	0,968	S-NPP = 20,02 + 4,40*AQUA	0.937
Breves	4.44	0,967	S-NPP = 171,01 + 3,06*AQUA	0.935
Ulianópolis	4.96	0,966	S-NPP = -72,72 + 5,3*AQUA	0.934
São Geraldo do Araguaia	6.04	0,965	S-NPP = 48,58 + 5,11*AQUA	0.932
Ourilândia do Norte	6.09	0,965	S-NPP = -105,99 + 6,53*AQUA	0.930
Brejo Grande do Araguaia	5.48	0,963	S-NPP = 38,17 + 4,06*AQUA	0.928
Dom Eliseu	5.02	0,963	S-NPP = -130 + 5,72*AQUA	0.928
Oriximiná	5.54	0,963	S-NPP = 74,41 + 5,36*AQUA	0.927
Senador José Porfírio	4.04	0,962	S-NPP = 83,84 + 3,81*AQUA	0.925
Parauapebas	4.89	0,960	S-NPP = -6,63 + 4,95*AQUA	0.922
Rurópolis	3.97	0,958	S-NPP = 83,65 + 3,79*AQUA	0.917
Alenquer	4.16	0,956	S-NPP = 161,18 + 3,79*AQUA	0.913
Paragominas	4.31	0,955	S-NPP = -934,56 + 6,22*AQUA	0.912
Garrafão do Norte	3.93	0,954	S-NPP = 165,85 + 2,5*AQUA	0.910
Porto de Moz	4.11	0,954	S-NPP = 26,84 + 4,04*AQUA	0.909
Aveiro	3.78	0,951	S-NPP = 110,11 + 3,5*AQUA	0.903
Anapu	3.98	0,950	S-NPP = -41,63 + 4,08*AQUA	0.902
Barcarena	3.7	0,949	S-NPP = 47,16 + 2,90*AQUA	0.900
São Sebastião da Boa Vista	3.48	0,947	S-NPP = 11,21 + 2,77*AQUA	0.898
Bragança	4.25	0,947	S-NPP = 146,86 + 2,82*AQUA	0.896
Itupiranga	4.79	0,947	S-NPP = 399,26 + 3,48*AQUA	0.896
Rio Maria	4.71	0,946	S-NPP = -64,15 + 5,24*AQUA	0.895
Bannach	5.69	0,945	S-NPP = 31,4 + 5,44*AQUA	0.894

Concórdia do Pará	3.89	0,944	S-NPP = 201,27 + 2,1*AQUA	0.891
Muaná	6.13	0,943	S-NPP = -48,09 + 6,86*AQUA	0.889
Uruará	4.21	0,941	S-NPP = -75,02 + 4,35*AQUA	0.885
Água Azul do Norte	5.11	0,939	S-NPP = -29,10 + 5,27*AQUA	0.882
Piçarra	5.74	0,939	S-NPP = 53,98 + 4,63*AQUA	0.882
Prainha	4.05	0,938	S-NPP = -89,12 + 4,24*AQUA	0.880
Melgaço	5.15	0,937	S-NPP = 93,08 + 3,48*AQUA	0.878
Limoeiro do Ajuru	2.86	0,937	S-NPP = 3,87 + 2,66*AQUA	0.877
Tucumã	5.1	0,936	S-NPP = 146,21 + 4*AQUA	0.876
Soure	5.92	0,935	S-NPP = 57,89 + 4,32*AQUA	0.875
Gurupá	3.54	0,935	S-NPP = -67,26 + 4,27*AQUA	0.874
Santa Cruz do Arari	5.19	0,932	S-NPP = 39,81 + 4,32*AQUA	0.868
Moju	3.94	0,931	S-NPP = 75,34 + 3,84*AQUA	0.867
Viseu	4.65	0,930	S-NPP = 86,52 + 4,11*AQUA	0.865
Cametá	4.13	0,929	S-NPP = 398,35 + 2,77*AQUA	0.863
Pau D'Arco	5.51	0,929	S-NPP = -113,28 + 6,79*AQUA	0.862
Tailândia	4.56	0,928	S-NPP = -169,79 + 5,32*AQUA	0.861
Cachoeira do Arari	5.88	0,927	S-NPP = 12,2 + 5,72*AQUA	0.860
Óbidos	4.39	0,927	S-NPP = 383,75 + 3,8*AQUA	0.860
Sapucaia	4.23	0,927	S-NPP = -0,01 + 4,23*AQUA	0.860
Terra Alta	4.05	0,927	S-NPP = 19 + 2,22*AQUA	0.860
Curralinho	3.77	0,926	S-NPP = 83,53 + 2,89*AQUA	0.858
Santa Izabel do Pará	5.54	0,926	S-NPP = 33,05 + 3,87*AQUA	0.858
Pacajá	4.09	0,925	S-NPP = 437,67 + 3,64*AQUA	0.856
Breu Branco	4.93	0,924	S-NPP = 138,13 + 3,74*AQUA	0.853
Floresta do Araguaia	5.35	0,923	S-NPP = 106,09 + 4,65*AQUA	0.851
Santa Maria do Pará	5.05	0,923	S-NPP = 45,68 + 3,08*AQUA	0.851
Curuá	4.18	0,921	S-NPP = -8,91 + 4,28*AQUA	0.849
Medicilândia	4.48	0,921	S-NPP = 35,4 + 4,35*AQUA	0.848
Castanhal	4.86	0,920	S-NPP = 30,75 + 4,14*AQUA	0.847
Bujaru	4.3	0,919	S-NPP = 288,46 + 2,58*AQUA	0.845
Jacundá	6.48	0,917	S-NPP = 48,13 + 4,93*AQUA	0.840
Placas	3.73	0,916	S-NPP = 244,80 + 3,32*AQUA	0.839
Nova Esperança do Piriá	4.25	0,915	S-NPP = 59,32 + 3,94*AQUA	0.837
Santa Luzia do Pará	4.58	0,914	S-NPP = 89,57 + 2,9*AQUA	0.836
Cachoeira do Piriá	5.06	0,912	S-NPP = -141,8 + 5,94*AQUA	0.832
Acará	3.91	0,912	S-NPP = 437,83 + 3,15*AQUA	0.831
Igarapé-Miri	3.6	0,911	S-NPP = 115,04 + 2,47*AQUA	0.831
Inhangapi	5.51	0,909	S-NPP = 39,78 + 3,6*AQUA	0.827
Oeiras do Pará	3.48	0,909	S-NPP = 161,75 + 2,78*AQUA	0.826
Irituia	5.21	0,907	S-NPP = 172,65 + 3,34*AQUA	0.822
Mojuí dos Campos	3.93	0,907	S-NPP = 211,83 + 3,3*AQUA	0.822
Santarém	4.2	0,907	S-NPP = 463,29 + 3,25*AQUA	0.822

São Domingos do Capim	4.58	0,906	S-NPP = 190,94 + 3,73*AQUA	0.821
Brasil Novo	5.12	0,904	S-NPP = 93,03 + 4,47*AQUA	0.818
Ipixuna do Pará	4.45	0,904	S-NPP = -59,77 + 4,71*AQUA	0.816
Novo Repartimento	5.23	0,900	S-NPP = 768,12 + 3,96*AQUA	0.810
Juruti	3.7	0,898	S-NPP = 277,05 + 2,54*AQUA	0.806
São Miguel do Guamá	5.19	0,896	S-NPP = 168,98 + 3,25*AQUA	0.803
Vitória do Xingu	5.34	0,887	S-NPP = -2,48 + 5,39*AQUA	0.787
Baião	4.29	0,873	S-NPP = 66,05 + 3,91*AQUA	0.762
Goianésia do Pará	4.73	0,872	S-NPP = 143 + 3,98*AQUA	0.761
Marapanim	3.91	0,872	S-NPP = 25,04 + 3,42*AQUA	0.760
Ponta de Pedras	7.82	0,872	S-NPP = 104,75 + 6,09*AQUA	0.760
Afuá	6.62	0,870	S-NPP = 11,55 + 5,13*AQUA	0.757
Monte Alegre	4.45	0,862	S-NPP = 74,57 + 4,26*AQUA	0.744
Portel	4.28	0,862	S-NPP = 295,77 + 3,97*AQUA	0.742
Palestina do Pará	6.43	0,860	S-NPP = 32,83 + 3,72*AQUA	0.739
São Caetano de Odivelas	3.98	0,856	S-NPP = 26,9 + 2,44*AQUA	0.732
Peixe-Boi	4.02	0,847	S-NPP = 33,41 + 2,24*AQUA	0.718
Bonito	3.67	0,841	S-NPP = 53,48 + 2,09*AQUA	0.707
Mocajuba	3.41	0,841	S-NPP = 146,09 + 2,2*AQUA	0.707
Belterra	4.1	0,838	S-NPP = 41,59 + 3,67*AQUA	0.703
Aurora do Pará	4.81	0,827	S-NPP = 146 + 3,58*AQUA	0.683
Tomé-Açu	4.27	0,824	S-NPP = 22,36 + 4,18*AQUA	0.679
Salvaterra	4.65	0,815	S-NPP = 60,07 + 3,3*AQUA	0.664
Igarapé-Açu	4.67	0,814	S-NPP = 36,97 + 3,48*AQUA	0.662
Capitão Poço	4.56	0,811	S-NPP = 160,82 + 3,29*AQUA	0.658
Bagre	3.66	0,808	S-NPP = 93,84 + 2,46*AQUA	0.652
Abel Figueiredo	5.51	0,807	S-NPP = 96,45 + 2,35*AQUA	0.651
Rondon do Pará	5.02	0,801	S-NPP = 690,63 + 2,8*AQUA	0.642
Augusto Corrêa	5.07	0,795	S-NPP = 129,29 + 2,46*AQUA	0.631
Faro	5.3	0,793	S-NPP = 35,04 + 4,14*AQUA	0.628
Nova Ipixuna	6.77	0,788	S-NPP = 100,26 + 4,58*AQUA	0.621
Capanema	4.11	0,778	S-NPP = 41,59 + 2,03*AQUA	0.605
Maracanã	4.22	0,776	S-NPP = 90,42 + 2,4*AQUA	0.603
Bom Jesus do Tocantins	6.21	0,776	S-NPP = 121,04 + 4,51*AQUA	0.602
Belém	7.11	0,769	S-NPP = 5,37+ 5,58*AQUA	0.591
Curuçá	4.05	0,768	S-NPP = 63,24 + 1,73*AQUA	0.591
São João de Pirabas	3.66	0,756*	S-NPP = 51,52 + 2,08*AQUA	0.572
Mãe do Rio	4.36	0,707*	S-NPP = 33,39 + 2,1*AQUA	0.500
Tucuruí	6.16	0,703*	S-NPP = 143,82 + 4,01*AQUA	0.494
Terra Santa	4.98	0,698*	S-NPP = 123,98 + 2,4*AQUA	0.487
Santo Antônio do Tauá	5.09	0,677*	S-NPP = 48,55 + 2,24*AQUA	0.458
Vigia	4.52	0,663*	S-NPP = 28,78 + 2,14*AQUA	0.439
Colares	5.14	0,658*	S-NPP = 24,91 + 2,14*AQUA	0.433

São Domingos do Araguaia	5.17	0,645*	S-NPP = 68,09 + 2,76*AQUA	0.417
São João da Ponta	4.34	0,618**	S-NPP = 30,29 + 1,42*AQUA	0.381
São Francisco do Pará	4.7	0,614**	S-NPP = 65,53 + 1,65*AQUA	0.377
Santarém Novo	3.99	0,592**	S-NPP = 26,94 + 1,89*AQUA	0.351
Ourém	4.77	0,584**	S-NPP = 77,65 + 1,81*AQUA	0.341
Salinópolis	3.86	0,549**	S-NPP = 11,4 + 2,08*AQUA	0.301
Magalhães Barata	3.43	0,534**	S-NPP = 43,25 + 1,39*AQUA	0.285
Tracuateua	4.1	0,510**	S-NPP = 65,88 + 1,89*AQUA	0.260
Benevides	5.64	0,436**	S-NPP = 9,23 + 1,44*AQUA	0.190
Nova Timboteua	4.92	0,407**	S-NPP = 51,28 + 1,99*AQUA	0.166
Santa Bárbara do Pará	8.84	0,286**	S-NPP = 19,76 + 2,67*AQUA	0.082
Quatipuru	**2.84**	0,280**	S-NPP = 24,42 + 0,45*AQUA	0.078
Primavera	3.92	0,268**	S-NPP = 44,83 + 0,87*AQUA	0.072
Ananindeua	**11.25**	0,156**	S-NPP = 4,17 + 0,83*AQUA	0.024
Marituba	6	-0,196**	S-NPP = 0,67 - 0,67*AQUA	0.038

Note: * p>0.01 and <0.05; ** p>0.05.

It was noticed that the absence of significative correlation was found only on small size municipalities. In fact, of the 11 smallest Pará's municipalities, only one of them presented a significative correlation (p<0.05) between AQUA and S-NPP yearly data (Figure 1).

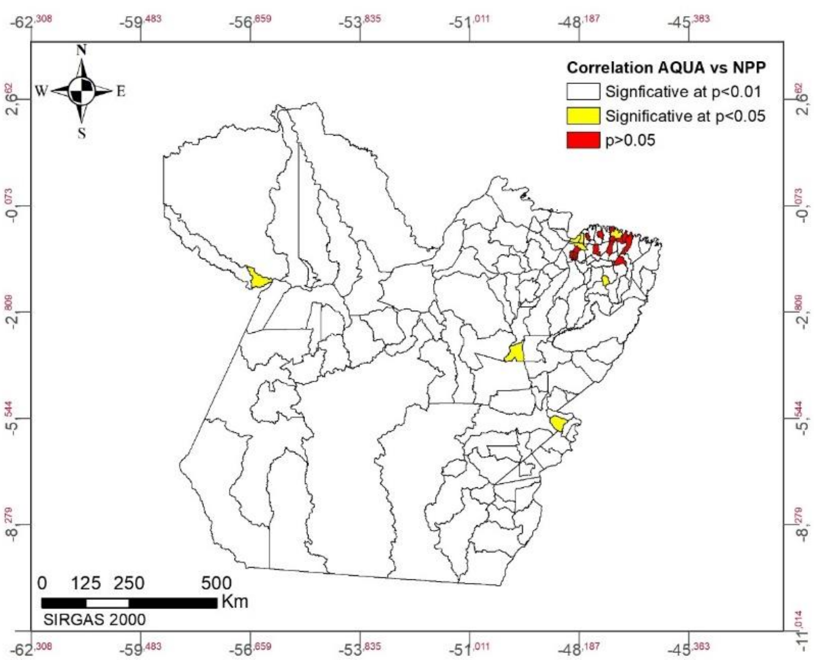

Figure 1 –Pará's municipalities highlighted according their p value of the AQUA vs S-NPP Person correlation.

4, Discussion

Fire detection omission (false negative) errors with the MODIS 1-km fire product happens more frequently than with the VIIRS 375 m (Coskuner, 2022; Fu et al., 2020; Vadrevu and Lasko, 2018; Waigl et al., 2017). This happens, mainly because the MODIS sensor has coarser spatial resolution than the VIIRS (Schroeder et al., 2014; Fu et al., 2020). Both, MODIS and VIIRS spectral bands at 4μm could contribute to the omission errors. This spectral band has been reported less sensitive than the shortwave infrared bands (e.g., 1.6μm) in detecting hotspots of gases flaring (Sharma et al., 2017).

Daytime commission (false positive) errors are typically found over bright land surfaces in areas of Sun glint predominantly associated with reflective rooftops on large industrial buildings. Nighttime commissions are largely associated with elliptical-shaped pixel clusters typical of active fire fronts, spatially coincident with known heat sources (e.g., active volcanoes, gas flares, iron mills), or scattered around active biomass burning areas (Schroeder et al., 2014). Since the VIIRS has greater resolution, commission errors are greater than on MODIS, once the first sensor detects more thermal anomalies that are not wildfire, when compared to the second (Waigl et al., 2017). Nevertheless, VIIRS 375 m commission errors are rare and usually accounts for less than 1.2% of the total (Schroeder et al., 2014).

High detection capability of the VIIRS relative to the MODIS has already been verified in previous studies. In Punjab, India, S-NPP fire pixels were higher by a factor of 4.8 compared to MODIS (AQUA and TERRA together) sensors data between 2012-2016. Taking into consideration only the AQUA satellite, the ratio rises to 6.5 (Vadrevu and Lasko, 2018). Coskuner (2022) counted a total of 54,154 fire pixels detected by the AQUA and TERRA satellites together during the period of 2015-2019 in Turkey, while the S-NPP detected a total of 211,511 fire pixels at the same location during the same period (VIIRS/MODIS ratio equal to 3.9). In a study done in Alaska, Waigl et al. (2017) concluded that there are, on average, 2.9 times the number of VIIRS detections for fire events as MODIS (AQUA and TERRA) detections. In the Northern Territory of Australia, in the 2016 fire season, Wickramasinghe et al. (2018) counted a total of 2,474 MODIS (AQUA and TERRA) fire pixels and 11,024 for VIIRS (VIIRS/MODIS ratio equal to 4.5). Lastly, in a case study done in Northeast Asia in November 6 of 2015, S-NPP detected 6,868 fire pixels, while both, AQUA and TERRA, detected 1,124 (VIIRS/MODIS ratio equal to 6.1) (Fu et al., 2020).

As seen above and based on the results found in this study, it is conclusive that the VIIRS detect more fire pixels than the MODIS sensor, but, the exact ratio it is not well stablished and, according to others works (eg. Fu et al., 2020; Waigl et al., 2017), depends on factors such as geographic area analyzed, the intensity of the fires, cloud conditions and timing of satellite overpasses. Differences between S-NPP and MODIS are further magnified due to coverage gaps along the tropics and sampling characteristics (pixel enlargement away from nadir) impacting the MODIS data (Schroeder and Giglio, 2017).

Especially in low-biomass lands (croplands, grasslands, and herbaceous vegetation) where the fires burn with low intensity, they are more likely to be detected only by the S-NPP satellite (Fu et al., 2020). Also, during night period, fires usually are more often detected by the VIIRS sensors due to its improved night-time fire detection algorithm (Schroeder and Giglio, 2017).

In this work, in particular, only data from the afternoon passage from the AQUA and S-NPP satellites was used. If the data from the night passages was used, it would be expected that the S-NPP/AQUA ratio increases.

As for the correlation between MODIS and VIIRS fire pixels, all studies found in the literature that analyzed this aspect, found a significative correlation between both data (Eg. Fu et al., 2020; Vadrevu and Lasko, 2018; Waigl et al., 2017). In this work, lack of significant correlation was found only in small size municipalities that together represented less than 0.5% of the fire pixels detected in the state of Pará. The size of these municipalities contributes to the result, since location errors can occur in satellite fire detection. For satellites with pixel resolution from 1 to 6 km, validation works indicate that the error on average is ~400 m, with a standard deviation of ~3 km. For the VIIRS sensors, the maximum error in accuracy is ~400 m (INPE, 2022). For a municipality such as Marituba, for example, that had the lowest number of fire pixels detected (1 from AQUA and 6 from S-NPP) and is Pará's smallest municipalities (103 km^2), a single location error, especially from the AQUA satellite, could considerably affect the correlation between both data.

4.Conclusions

This study contributes to a better understanding of the performance in fire detection between AQUA (MODIS - Collection 6) and S-NPP (VIIRS - VNP14IMG), providing valuable information for their application in fire identification.

Based on the results found, in general, for each fire pixel detected by the AQUA satellite during the afternoon passage over the South America continent, 5.13 fire pixels are detected by the S-NPP satellite during the afternoon passage at the same continent. This relationship changes from country to country especially in small locations.

Overall, the correlation between AQUA and S-NPP data were significant, except in small locations with low fire incidence. Therefore, fire detection data in these places should be carefully analyzed. For larger areas with high detection of fire pixels, linear regression equation could be used to convert S-NPP data to AQUA or vice-versa, when the AQUA satellite stops providing data.

Additional studies could be carried out to better understand the factors that interfere in the detection of active fire pixels by MODIS and VIIRS sensors.

Acknowledgements

To Jamile Alves dos Santos for the help in the data collect, to professor Theodore James White for providing language help, to PROPES from IFBaiano and to CNPq for the PIBIC EM scholarship.

References

Badarinath, K. V. S.; Sharma, A. R.; Kharol, S. K. Forest fire monitoring and burnt area mapping using satellite data: a study over the forest region of Kerala State, India. International Journal of Remote Sensing, v. 32, n. 1, p. 85-102, 2011. DOI: https://doi.org/10.1080/01431160903439890

Cao, C.; Deluccia, F.; Xiong, X.; Wolfe, R.; WENG, F. Early On-orbit Performance of the Visible Infrared Imaging Radiometer Suite (VIIRS) onboard the Suomi National Polar-orbiting Partnership (S-NPP) Satellite. IEEE Transactions on Geoscience and Remote Sensing, v. 52, n. 2, p. 1142-1156, 2013. DOI: https://doi.org/10.1109/TGRS.2013.2247768

Csiszar, I.; Denis, L.; Giglio, L.; Justice, C. O.; Hewson, J. Global fire activity from two years of MODIS data. International Journal of Wildland Fire, v. 14, n. 2, p. 117-130, 2005. DOI: https://doi.org/10.1071/WF03078

Csiszar, I.; Morisette, J. T.; GIGLIO, L. Validation of active fire detection from moderate-resolution satellite sensors: The MODIS example in Northern Eurasia. IEEE Transactions on Geoscience and Remote Sensing, v. 44, n. 7, p. 1757-1764, 2006. DOI: https://doi.org/10.1109/TGRS.2006.875941

Csiszar, I.; Schroeder, W.; Giglio, L.; Ellicott, E.; Vadrevu, K. P.; Justice, C. O.; WIND, B. Active fires from the Suomi NPP Visible Infrared Imaging Radiometer Suite: Product status and first evaluation results. Journal of Geophysical Research: Atmospheres, v. 119, n. 2, p. 803–816, 2014. DOI: https://doi.org/10.1002/2013JD020453

Fu, Y.; LI, R.; WANG, X.; BERGERON, Y.; VALERIA, O.; CHAVARDÈS, R. D.; WANG, Y.; HU, J. Fire detection and fire radiative power in forests and low-biomass lands in Northeast Asia: MODIS versus VIIRS fire products. Remote Sensing, v. 12, n. 18, p. 2870, 2020. DOI: https://doi.org/10.3390/rs12182870

Giglio, L.; CsiszaR, I.; Justice, C. O. Global distribution and seasonality of active fires as observed with the Terra and Aqua Moderate Resolution Imaging Spectroradiometer (MODIS) sensors. Journal of geophysical research: Biogeosciences, v. 111, n. G2, 2006. DOI: https://doi.org/10.1029/2005JG000142

Giglio, L.; Schroeder, W.; Hall, J. V.; JUSTICE, C. O. Modis collection 6 active fire product user’s guide: Revision B. Department of Geographical Sciences. University of Maryland, 9, 2018. Available at: https://www.earthdata.nasa.gov/s3fs-public/imported/MODIS_C6_Fire_User_Guide_B.pdf Accessed on November 2, 2022.

Hawbaker, T. J.; Radeloff, V. C.; Syphard, A. D.; Zhu, Z.; Stewart, S. I. Detection rates of the MODIS active fire product in the United States. Remote Sensing of Environment, v. 112, n. 5, p. 2656-2664, 2008. DOI: https://doi.org/10.1016/j.rse.2007.12.008

INPE - Instituto Nacional de Pesquisas Espaciais. Portal do Monitoramento de Queimadas e Incêndios. 2022. Available at: http://www.inpe.br/queimadas Accessed on 02 Jan. 2022.

Li, F.; zhang, X.; Kondragunta, S.; CSISZAR, I. Comparison of fire radiative power estimates from VIIRS and MODIS observations. Journal of Geophysical Research: Atmospheres, v. 123, n. 9, p. 4545-4563, 2018. DOI: https://doi.org/10.1029/2017JD027823

NASA - National Aeronautics and Space Administration. VNP14IMG - VIIRS/NPP Active Fires 6-Min L2 Swath 375m. 2022. Available at: https://ladsweb.modaps.eosdis.nasa.gov/missions-and-measurements/products/VNP14IMG Accessed on May 5, 2022.

Schroeder, W.; Giglio, L. NASA VIIRS Land Science Investigator Processing System (SIPS) Visible Infrared Imaging Radiometer Suite (VIIRS) 375 m & 750 m Active Fire Products. Product User's Guide Version 1.4. University of Maryland: NASA, 2017. Available at: https://lpdaac.usgs.gov/documents/132/VNP14_User_Guide_v1.3.pdf Accessed on July 23 2022.

Sharma, A.; Wang, J.; Lennartson, E.M. Intercomparison of MODIS and VIIRS fire products in Khanty-Mansiysk Russia: Implications for characterizing gas flaring from space. Atmosphere, v. 8, n. 6, p. 1-19, 2017. DOI: https://doi.org/10.3390/atmos8060095

Vadrevu, K.; Lasko, K. Intercomparison of MODIS AQUA and VIIRS I-Band fires and emissions in an agricultural landscape—Implications for air pollution research. Remote Sensing, v. 10, n. 7, 978, 2018. DOI: https://doi.org/10.3390/rs10070978

Xia, X.; Zong, X.; Sun, L. Exceptionally active agricultural fire season in mid-eastern China in June 2012 and its impact on the atmospheric environment. Journal of Geophysical Research: Atmospheres, v. 118, n. 17, p. 9889-9900, 2013. DOI: https://doi.org/10.1002/jgrd.50770

Waigl, C. F., Stuefer, M., Prakash, A., & ICHOKU, C. Detecting high and low-intensity fires in Alaska using VIIRS I-band data: An improved operational approach for high latitudes. Remote Sensing of Environment, v. 199, n. 2017, p. 389-400, 2017. DOI: https://doi.org/10.1016/j.rse.2017.07.003

White, B. L. A. Satellite detection of wildland fires in South America. Floresta, v. 49, n. 4, p. 851-858, 2019. DOI: http://dx.doi.org/10.5380/rf.v49i4.60117

White, B. L. A. Spatiotemporal variation of fire occurrence in the State of Bahia, Brazil, between 2003 and 2019. Journal of Hyperspectral Remote Sensing, v. 10, n. 3, p. 153-167, 2020. DOI: https://doi.org/10.29150/jhrs.v10.3.p153-167

White, B. L. A.; White, L. A. S. Queimadas e incêndios florestais no estado de Sergipe, Brasil, entre 1999 e 2015. Floresta, v. 46, n. 4, p. 561-570, 2017. DOI: http://dx.doi.org/10.5380/rf.v46i4.47036

Wickramasinghe, C.; WALLACE, L.; REINKE, K.; JONES, S. Intercomparison of Himawari-8 AHI-FSA with MODIS and VIIRS active fire products. International Journal of Digital Earth, v. 13, n. 4, p. 457-473, 2020. DOI: http://dx.doi.org/10.1080/17538947.2018.1527402